Electronic Supplementary Information (ESI)

Bone-repair properties of biodegradable hydroxyapatite nano-rods superstructures

Noelia L. D' Elía[(a)], Colleen Mathieu[(b)], Caroline D. Hoemann[(b, c, d)], Juan A. Laiuppa[(e)], Graciela E. Santillan[(e)], Paula V. Messina*[(a)].

(a) Department of Chemistry, Universidad Nacional del Sur, (8000) Bahía Blanca, Argentina. INQUISUR-CONICET. (b) Institute of Biomedical Engineering, École Polytechnique, Montréal, QC, Canada. (c) Groupe de Recherche en Sciences et Technologies Biomédicales (GRSTB), Canada. (d) Department of Chemical Engineering, École Polytechnique, Montréal, QC, Canada. (e) Department of Biology, Biochemistry and Pharmacy, Universidad Nacional del Sur, (8000) Bahía Blanca, Argentina.

* Author to whom correspondence should be addressed. Tel: +54 291 4595159. Fax: +54 291 4595160. Electronic mail: pmessina@uns.edu.ar.

Single roughness depth ($R_{Z,i}$); the maximum roughness depth ($R_{Z,max}$) and the mean roughness depth ($R_{Z,mean}$) parameters. Examples of $R_{z,i}$ are indicated in materials roughness profiles.

Figure 1 ESI: MI surface roughness profile.

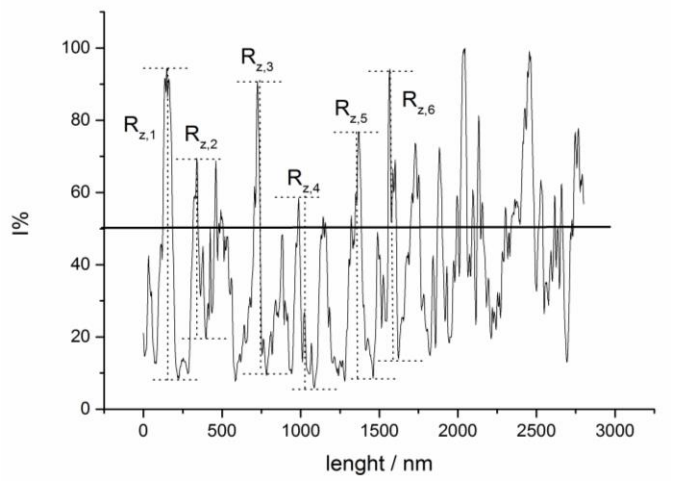

$R_{z,\ mean}$	SD	Minimum	Median	$R_{z,\ max}$
56.7	**14.4**	**27.3**	**58.5**	**85**

Figure 2 ESI: MII surface roughness profile.

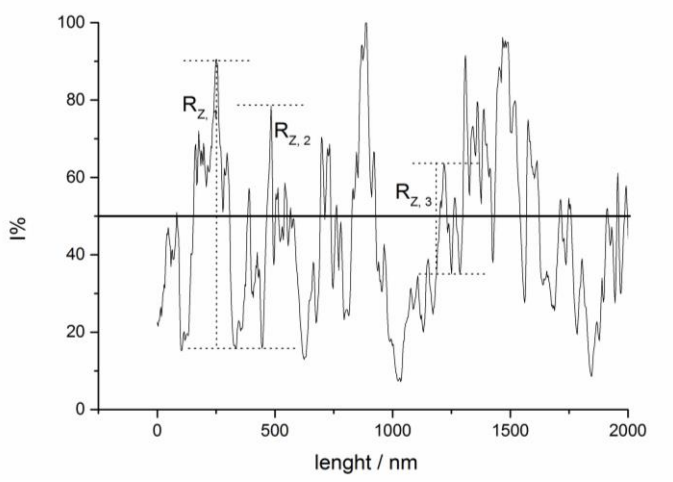

$R_{z,\ mean}$	SD	Minimum	Median	$R_{z,\ max}$
42.9	**28.1**	**9.2**	**35.9**	**91.5**

Figure 3 ESI: MIII surface roughness profile.

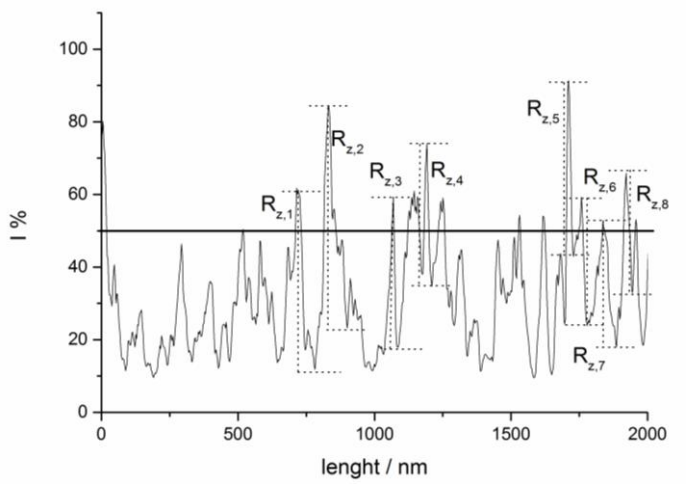

$R_{z,\ mean}$	SD	Minimum	Median	$R_{z,\ max}$
38.7	**11.7**	**20.9**	**36.3**	**71.7**

Figure 4 ESI: MIV surface roughness profile.

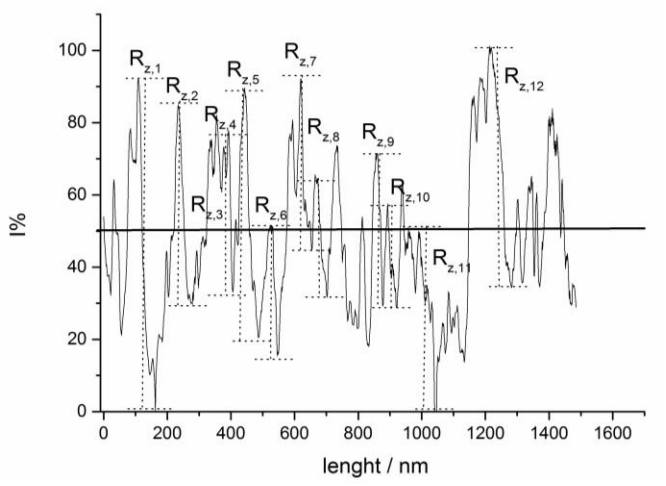

$R_{z,\ mean}$	SD	Minimum	Median	$R_{z,\ max}$
40.8	**21.6**	**7.4**	**37.9**	**90,7**

Figure 5 ESI: Nano-hydroxyapatite superstructures degradation in physiological fluid conditions (phosphate buffer saline, pH = 7.4). At 36°C all materials exhibited a weight loss minor than 2.5%; while at 25°C no degradation can be recorded.

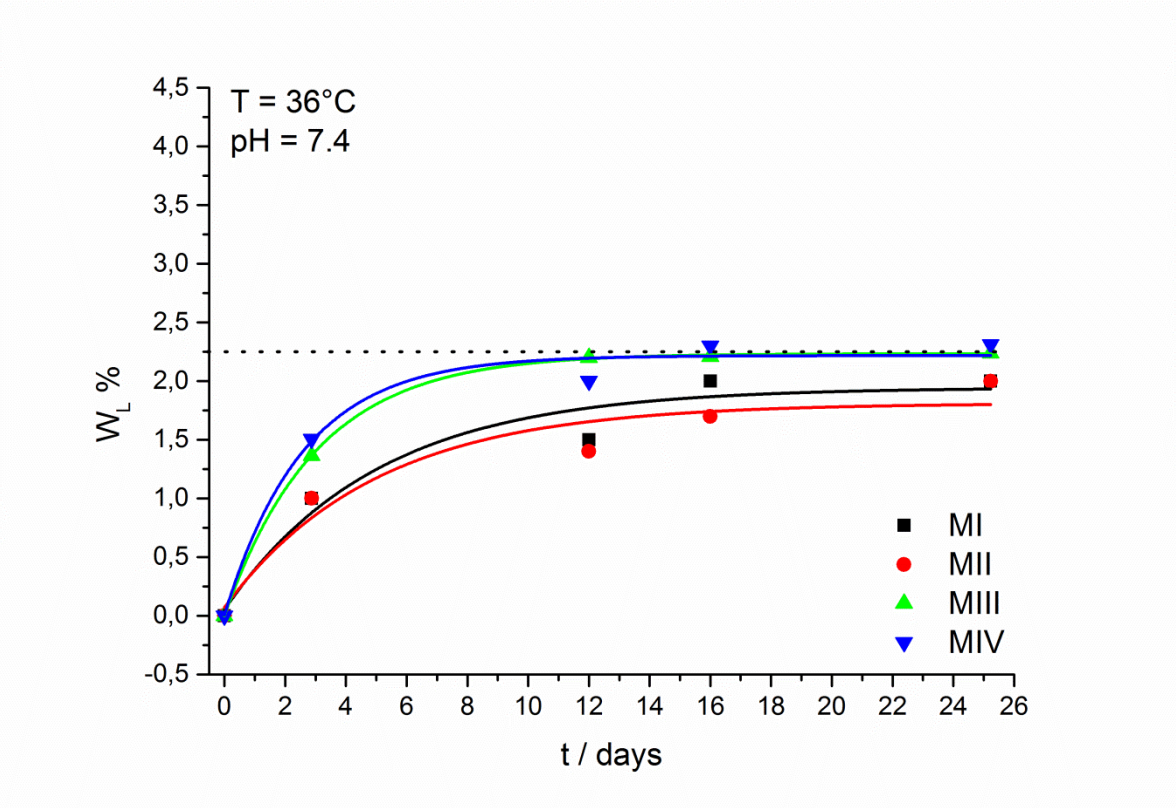

Figure 6 ESI: Optical microphotographs showing MSCs adhesion on the nano-HAp powder coatings (MI, MII, MIII and MIV) with different nanoparticles amounts. At high amount of nano-HAp (3100 μg/cm^2) non-adherent cells are observed.

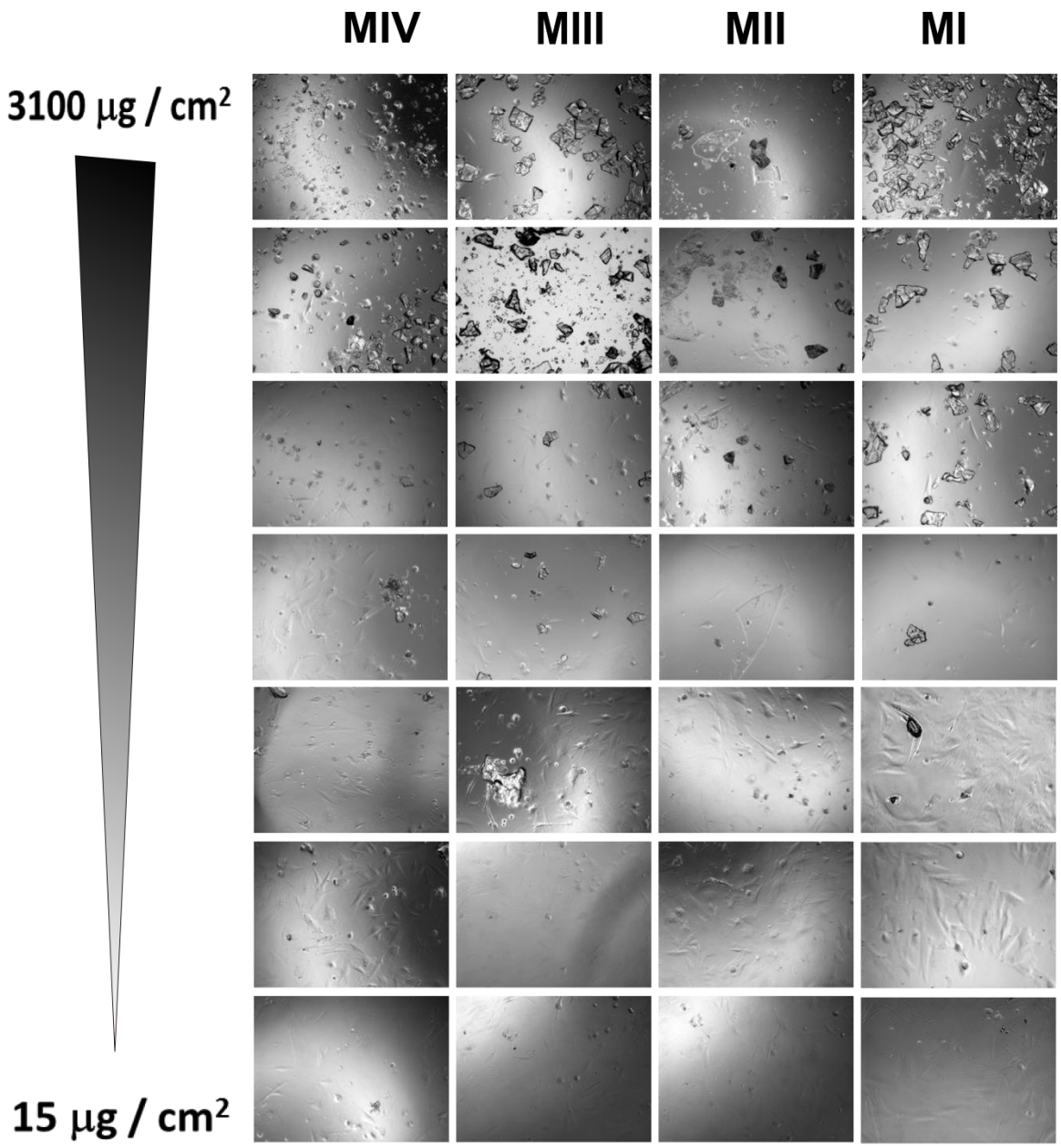

Figure 7 ESI: Optical microphotographs showing MSCs morphology after adhesion on Co-I; MI/ Co-I coatings and non-coated glass slide used as positive control (C+). [(1)] Co- I (31 μg / cm^2); [(2)] HAp (MI) 7200 μg/cm^2. **Slide A:** A1, A2 cell adhesion on Co-I coating; A4, A5 example area with high mineral concentration and no visible adherent cells. **Slide B:** adherent cells on C+. **Slide C:** C1, C5 adherent cells on Co-I coatings; C2, C6 example area with high mineral concentration and no visible adherent cells; C3, C7 adherent cells on C+.

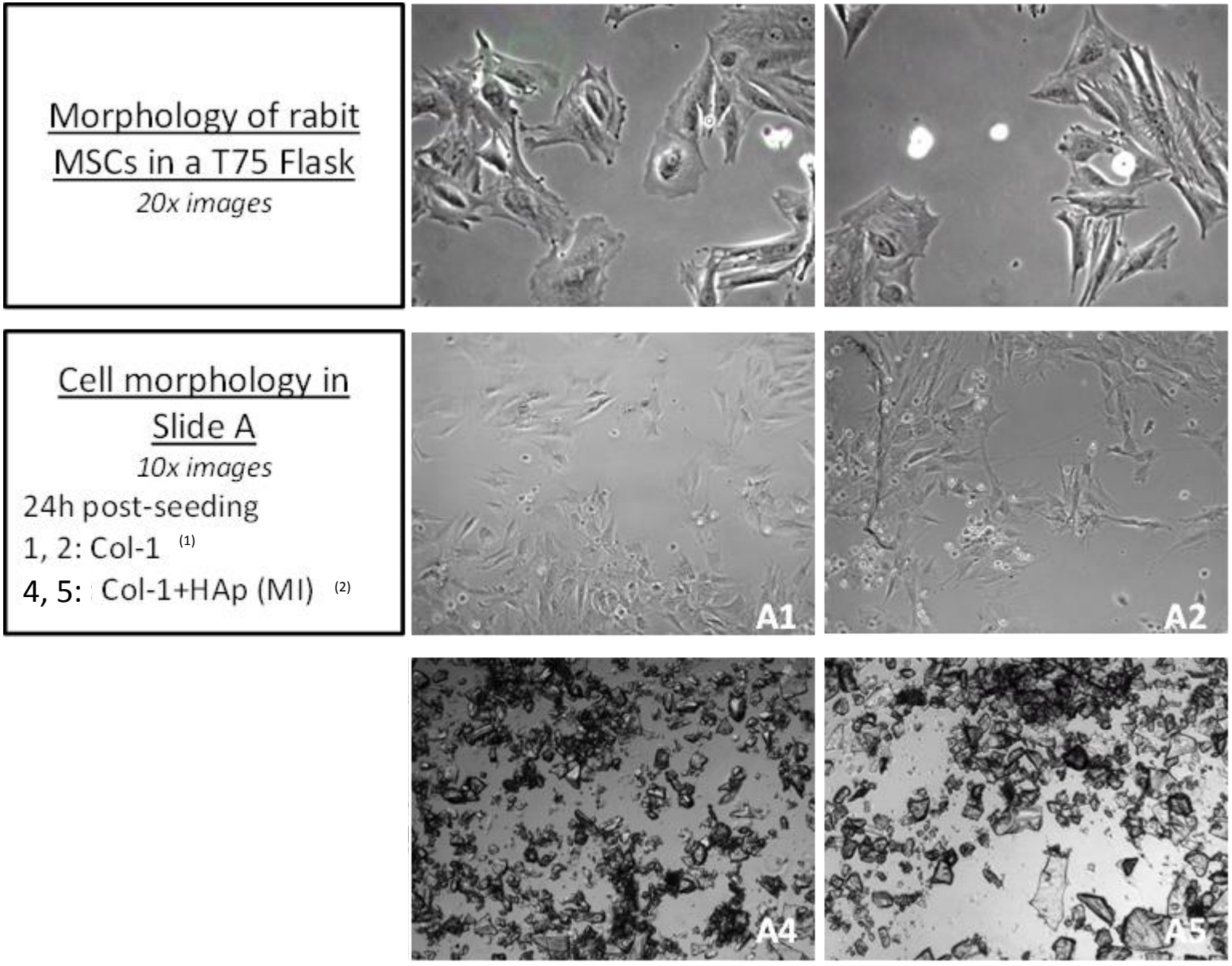

Cell morphology in Slide B

10x images

24h post-seeding

1→4: None (glass)

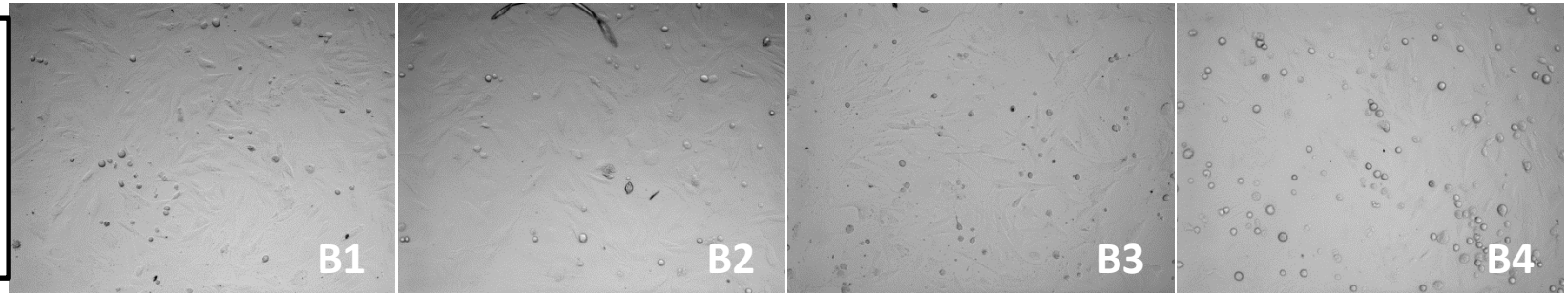

Cell morphology in Slide C

10x images

24h post-seeding

Controls:

1&5: Co I [(1)]

2&6: Co I/HA [(2)]

3&7: None (glass)

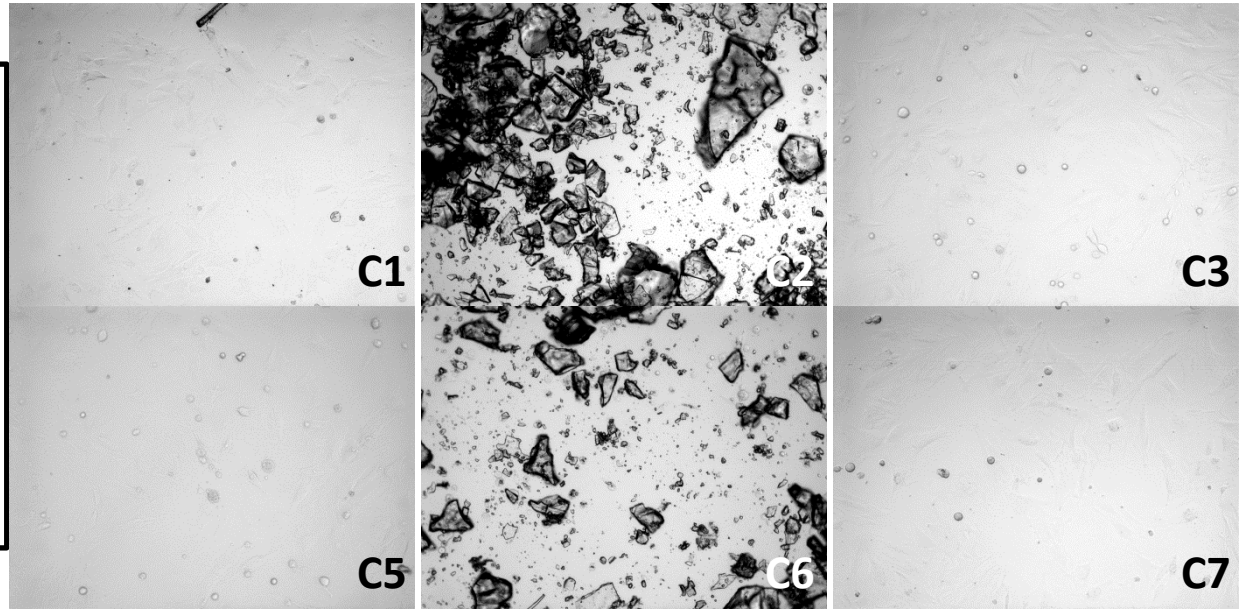

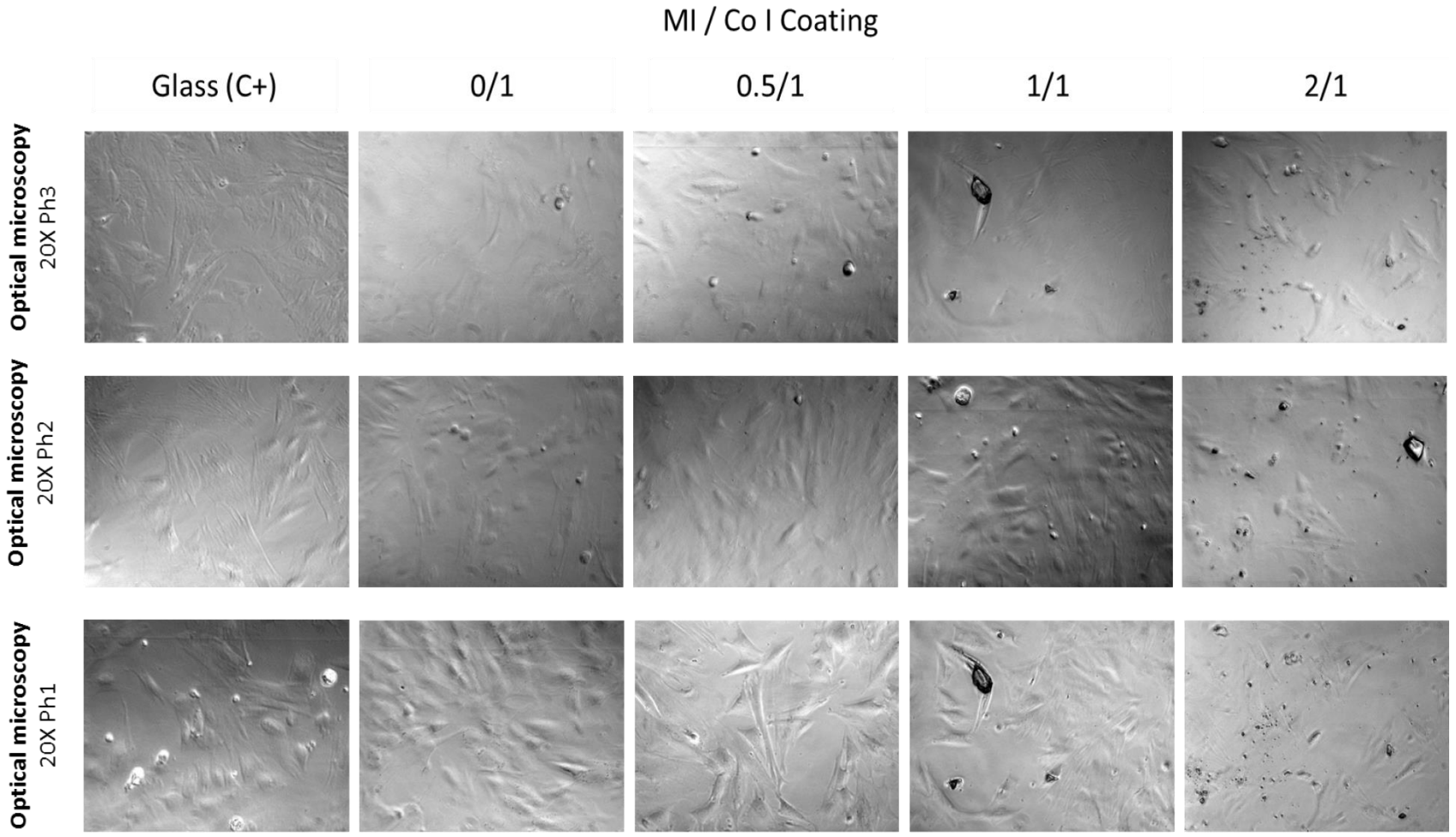
MI / Co I Coating
Glass (C+)
0/1
0.5/1
1/1
2/1
Optical microscopy
20X Ph3
Optical microscopy
20X Ph2
Optical microscopy
20X Ph1

Figure 8 ESI: Laser scanning confocal microphotographs showing MSCs α-SMA expression using large amounts of hydroxyapatite MI (7200 µg/cm^2) / Co I (31 µg/cm^2) coatings to test cytotoxicity.

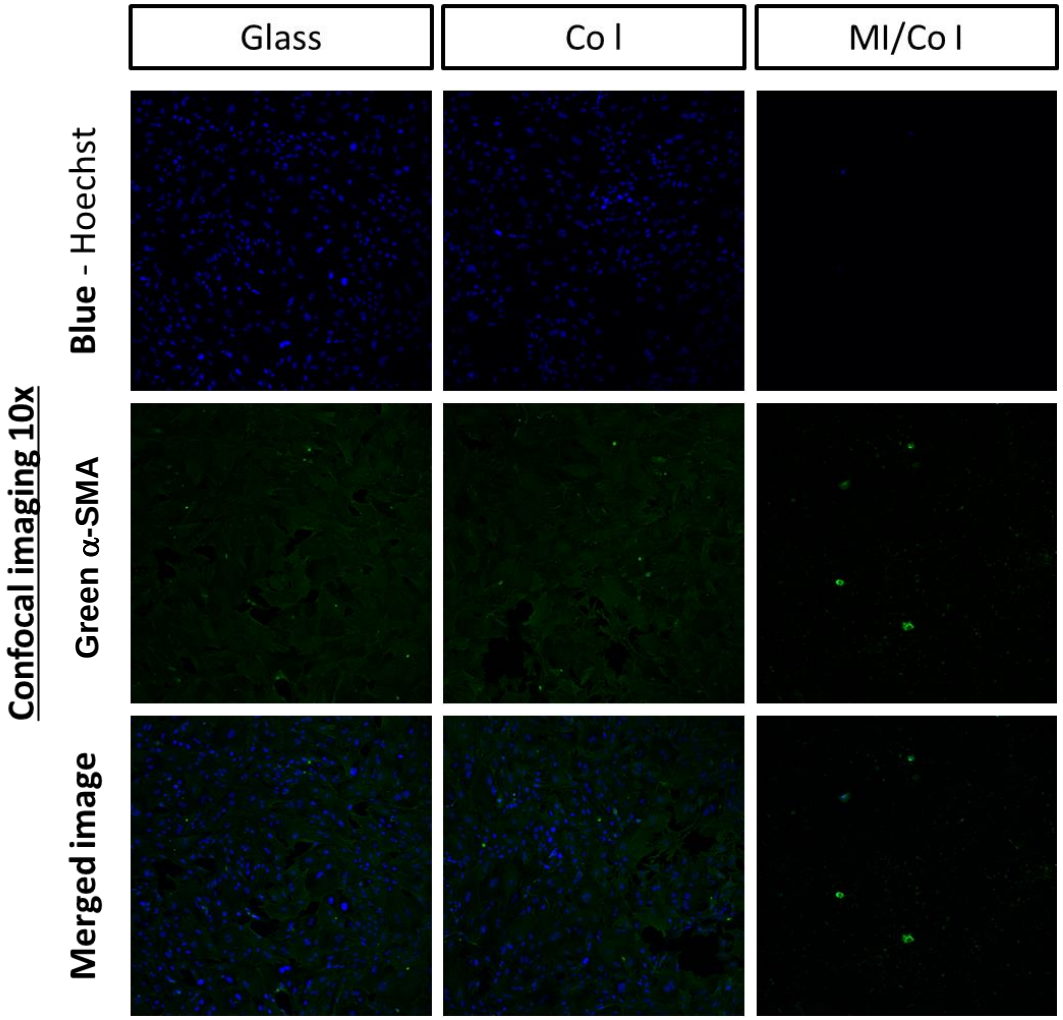

Figure 9 ESI: Figure 10 (a) supplementary information. Immunofluorescence assay: confocal microphotographs 10×. The bar graph shows the number of nucleus counted by Image J software in each replicate slide. Non-coated glass slide was used as positive control (C+).

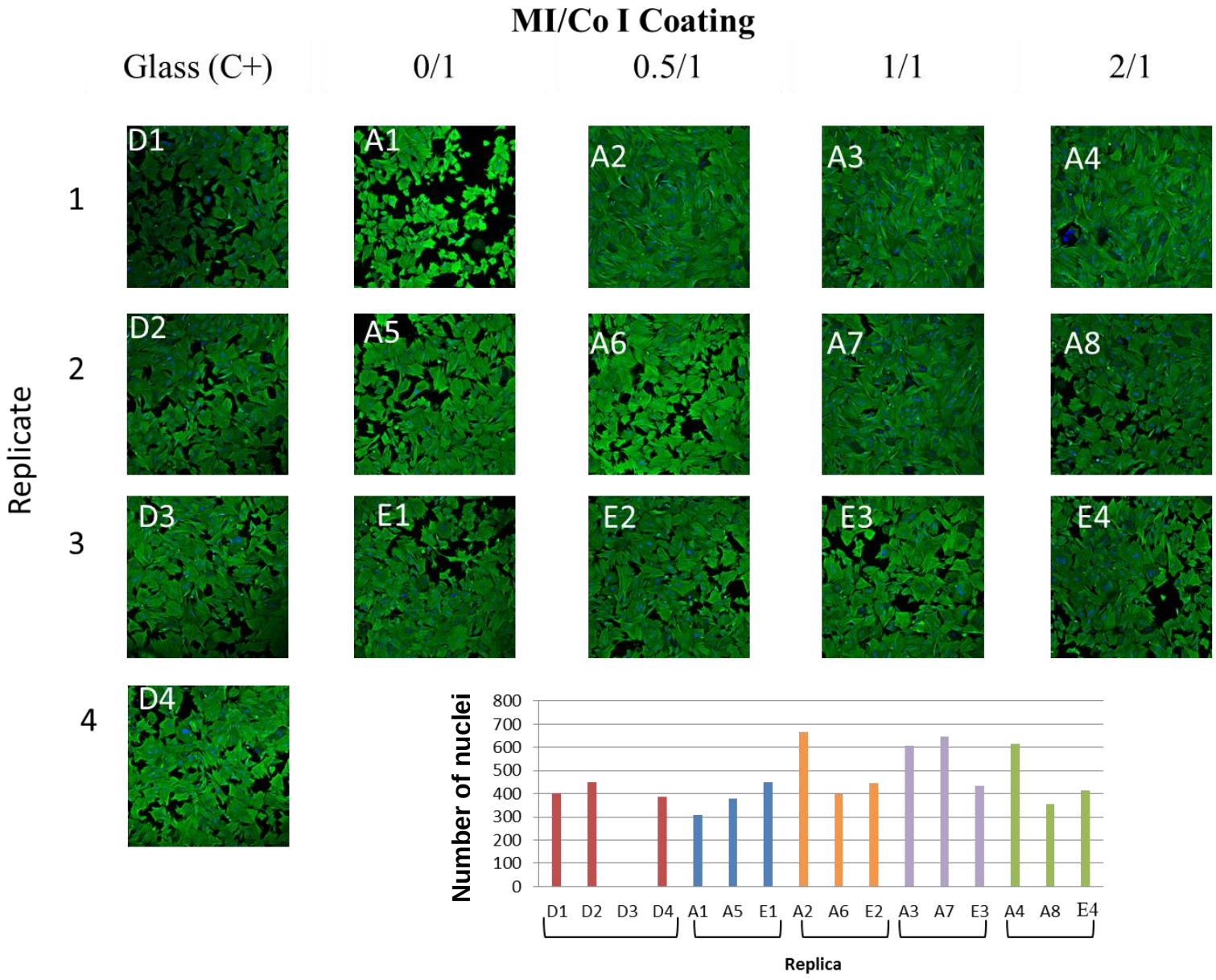

Figure 10 ESI: Image analysis for α-SMA expression (monochromatic image, green laser 488nm), the mean green pixel intensity was determined from the mean brightness value of all green pixels analyzed per image. Supplementary information of methodology section 2.7.3: "*MSC actin-based spreading on Collagen type I without and with nano-Hap /: Immunofluorescence confocal microscopy".*